THE JOURNAL OF PHYSICAL CHEMISTRY LETTERS
A JOURNAL OF THE AMERICAN CHEMICAL SOCIETY

pubs.acs.org/JPCL

Letter

Molecular Mechanism of Cell Membrane Protection by Sugars: A Study of Interfacial H-Bond Networks

Xiao You, Euihyun Lee, Cong Xu, and Carlos R. Baiz*

Cite This: *J. Phys. Chem. Lett.* 2021, 12, 9602–9607

Read Online

ACCESS | Metrics & More | Article Recommendations | Supporting Information

ABSTRACT: Sugars function as bioprotectants by stabilizing biomolecules during dehydration, thermal stress, and freeze–thaw cycles. A buildup of sugars occurs in many organisms upon their exposure to extreme conditions. Understanding sugar's bioprotective effects on membranes is achieved by characterizing the H-bond networks at the lipid–water interface. Here, we report the headgroup H-bond populations, structures, and dynamics of 1,2-dimyristoyl-*sn*-glycero-3-phosphocholine vesicles in concentrated glucose solutions using ultrafast two-dimensional infrared spectroscopy in conjunction with molecular dynamics simulations. H-Bond populations and dynamics at the ester carbonyl positions are largely unaffected even at very high, 600 mg/mL, sugar concentrations. In addition, dynamics exhibit a slight nonmonotonic dependence on sugar concentration. Simulations, which are in near-quantitative agreement with measured dynamics, show that the H-bond structure remains largely intact by the existence of sugar. This study shows that the bioprotection of sugar is realized through stable lipid–saccharide–water H-bond networks at the membrane interface that mimic the H-bond networks in pure water.

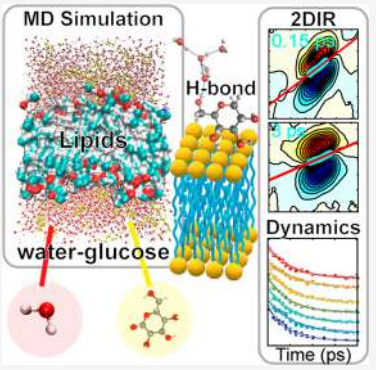

Robust organisms such as yeasts, nematodes, and resurrection plants naturally survive extreme conditions such as dehydration, thermal stress, and freeze–thaw cycles. In particular, dehydration is linked to high concentrations of sugars, which can be up to 20% of the dry weight of certain species.[2] Thermodynamic, spectroscopic, and simulation studies have attributed the bioprotection mechanism to the stabilization of biomolecules in general and lipid membranes in particular, where sugars protect membranes against fusion and leakage.[3−11] For example, trehalose, a disaccharide of glucose, preserves the melting transition of highly dehydrated lipid bilayers.[9,12,13]

Despite substantial efforts, sugar–lipid interactions have been challenging to describe, and as consequence, there are several outstanding questions.[3,4,14,15] (1) How do sugars impact the interfacial H-bond networks, and how does this affect the functional characteristics of membranes? (2) What is the specific dehydration protection mechanism? Specifically, do sugars mimic the interfacial environment of water or generate unique environments under dehydration conditions? The water replacement hypothesis suggests that sugar protects lipids during dehydration by directly interacting with the lipid headgroups and preserving the structural integrity of the membrane at dehydration concentrations. Certain structural aspects of water's interfacial H-bond network are mimicked by the sugar through the hydroxyl groups, creating an environment that supports similar lipid–lipid interactions that result in bilayer stabilities that are similar to the fully hydrated system.[16,17] This theory is supported by molecular dynamics (MD) simulations, nuclear magnetic resonance (NMR), and fluorescence microscopy,[18,19] with other evidence supporting the presence of an entropy-driven phase transition in which sugars become depleted from the interface at high concentrations.[4,8,20−22] These models, however, must be assessed by carefully examining the structure and dynamics (lifetimes) of the complex H-bond networks at the lipid–sugar–water interface because populations and thermodynamics alone remain insufficient to describe their stabilizing mechanisms.

Lipid bilayers create a complex network of interfacial H-bonds that is markedly different from bulk water as a result of strong polar interactions within the lipid headgroups.[23−26] Understanding how sugars modulate interfacial environments also requires contrasting them with the H-bond networks in the bulk. In this study, we measure the H-bond populations and dynamics at the lipid–water interface, as well as in bulk, over a range of glucose concentrations. We use a combination of Fourier-transform infrared (FTIR) spectroscopy and ultrafast two-dimensional infrared (2D IR) spectroscopy.[27] Specifically, we probe the ester carbonyl stretching modes of 1,2-dimyristoyl-*sn*-glycero-3-phosphocholine (DMPC), a well-studied phospholipid (Figure 1A); these groups are located precisely at the hydrophobic–hydrophilic interface (Figure

Received: July 27, 2021
Accepted: September 21, 2021
Published: September 29, 2021

https://doi.org/10.1021/acs.jpclett.1c02451
J. Phys. Chem. Lett. 2021, 12, 9602–9607

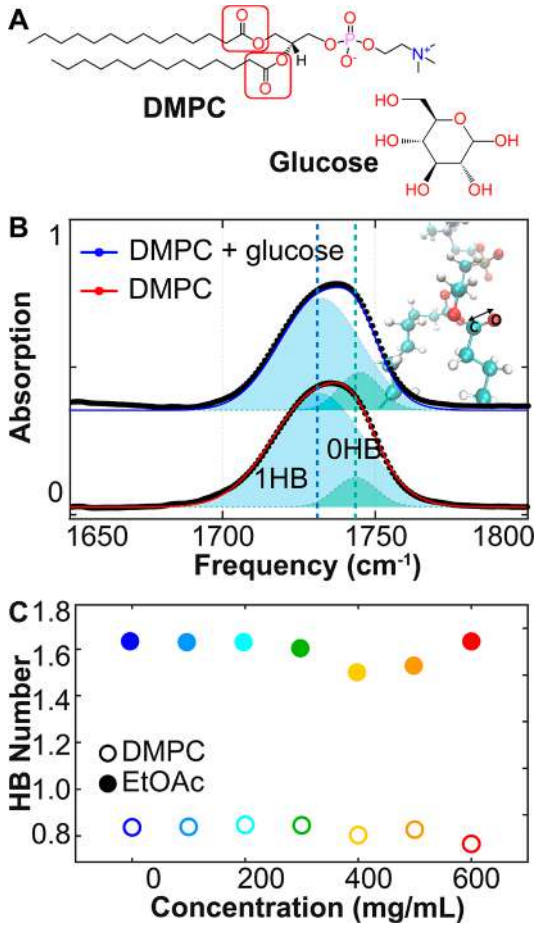

Figure 1. (A) Structures of DMPC and glucose. (B) Normalized carbonyl absorption spectra of 100 nm DMPC vesicles in pure D_2O (red) and a 600 mg/mL glucose solution (blue). The carbonyl band is well represented by two peaks that correspond to the zero- and one-H-bond ensembles, respectively. (C) Average number of H-bonds to each carbonyl group form in DMPC and EtOAc solutions across the sugar concentration range extracted by the oscillator strength-weighted ($\varepsilon_{1HB}/\varepsilon_{0HB}$ = 1.49) areas of the two peaks as described previously.[1]

S12). Dynamics in bulk solution are measured using ethyl acetate, a small water-soluble vibrational probe (Section S2). Experiments are interpreted through MD simulations, which provide atomistic descriptions of the H-bond networks.

The H-bond dynamics of lipids under varying conditions have been characterized with FTIR and 2D IR methods.[1,23,27−30] Specifically, the carbonyl stretching band (~1700−1750 cm^{-1}) is described by a combination of two Gaussian peaks, assigned to zero-H-bond (peak I) and one-H-bond (peak II) ensembles as shown in Figure 1B.[31] The H-bond populations are proportional to the peak I and peak II areas weighted by their oscillator strength.[1] Surprisingly, there is no change in peak ratios with an increase in glucose concentration (Figure S1), showing that the fraction of H-bonded carbonyls remains unaffected throughout the concentration range, despite the high glucose concentrations of ≤600 mg/mL.

Temperature-dependent FTIR measurements provide access to H-bond thermodynamics.[25,27,31−34] An increased glucose concentration decreases the H-bond enthalpy (Figure S4A) from 12.5 ± 0.2 kJ/mol in bulk water to 7.8 ± 0.5 kJ/mol in 300 mg/mL glucose. However, the trend is nonmonotonic, with a further increase to 9.8 ± 1.7 kJ/mol at 600 mg/mL glucose. The trends indicate that the sugar−lipid H-bonds are stronger than the water−lipid H-bonds as the process is observed to be less endothermic. The observed enthalpic changes, however, are relatively low when compared to that of a carbonyl probe in the bulk (Figure S4B), which in fact change magnitude from 4.3 ± 1.4 kJ/mol in bulk water to −6.0 ± 0.6 kJ/mol in 600 mg/mL glucose. Given that these experimentally measured enthalpies do not differentiate lipid−sugar H-bonds from lipid−water H-bonds, these values reflect the H-bond strength weighted by the fractions of sugar and water H-bonds to the lipids over the concentration range. Together, these results show that the glucose has only minor effects on the lipid−water interface hydration and enthalpy compared to the bulk, indicating that the interfacial H-bond networks remain largely intact even at very high sugar concentrations.

H-Bond dynamics are extracted from measured 2D IR spectra. The evolution of the line shapes as a function of waiting time provides a frequency−frequency correlation function (FFCF) exponential relaxation time constant via a nodal line slope (NLS) analysis of the ester carbonyl 2D IR spectra (Figure 2A,B and section S3).[23] Surprisingly, the measured decay time of 1.23 ps at 600 mg/mL is identical, within error, to the pure water value of 1.19 ps, indicating that interfacial H-bond dynamics are largely unperturbed despite the high sugar concentration. These measurements indicate that the H-bond networks at the interface remain largely intact across a very wide concentration range. Despite the small variation in dynamics, there are some nuances in the observed trends. Dynamics become slightly faster at intermediate glucose concentrations; for example, the time constant decreases from 1.36 to 1.06 ps between 100 and 300 mg/mL glucose (Figure 2C), and a deceleration is observed above 300 mg/mL. These experimentally measured dynamics are in agreement with the computed FFCF from the MD trajectories using a vibrational map (section S5),[31] which similarly show a nonmonotonic dependence of the exponential time constant (Figure 2C). Nonmonotonic trends in dynamics at membrane interfaces have been reported previously in DMPC vesicles in co-solvent systems, as well as a function of transmembrane crowding. The results are interpreted in terms of opposing effects, which become dominant in different concentration regimes.[29,35]

The ethyl acetate carbonyl stretch in a glucose-crowded solution probes the H-bond of bulk water. The relaxation of bulk water is 2 times faster than that of interfacial water (Figure 2C,D). Similar to the interface, the glucose crowder produces only a small increase in dynamics, from 0.55 ps in pure water to 0.71 ps at 400 mg/mL glucose, a 30% deceleration of dynamics. However, considering that the bulk viscosity in 600 mg/mL glucose solutions increases 4-fold versus that of pure water,[36] the measured deceleration in the H-bond dynamics indicates that, at the molecular level, the effects of sugar on H-bond dynamics are insignificant. Water diffusion rates computed from MD simulations (Figure S20) suggest an ~2−3-fold deceleration in dynamics between pure water and the highest sugar concentration, and this deceleration is very similar at the lipid−water interface and the bulk.

Similar to experiments, MD simulations predict a small but nonmonotonic trend in H-bond dynamics with an increase in

https://doi.org/10.1021/acs.jpclett.1c02451
J. Phys. Chem. Lett. 2021, 12, 9602−9607

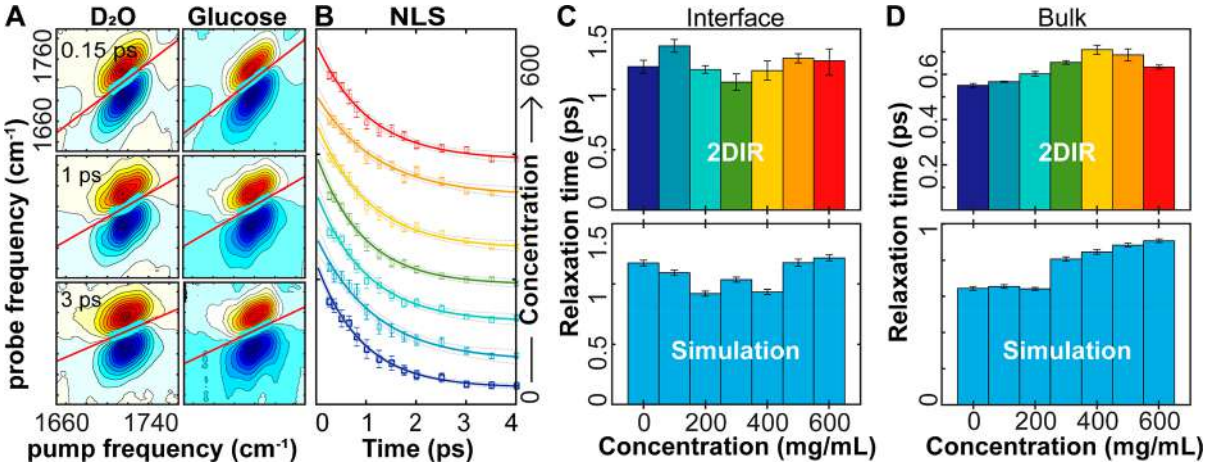

Figure 2. (A) Representative 2D IR spectra of the DMPC carbonyl stretching mode in D_2O and in a 600 mg/mL glucose solution at three waiting times to show the decrease in diagonal elongation. (B) Nodal line slope decays of DMPC in glucose solutions extracted from 2D IR spectra in Figures S5−S11 along with single-exponential fits. (C) Single-exponential decay constants extracted from fits to the experimentally measured NLS decay (B, solid lines) and decay constants extracted from frequency−frequency correlation functions computed from MD trajectories as described in section S5 of the Supporting Information. (D) Similarly, exponential decay constants of ethyl acetate carbonyl in the same sucrose solutions measured as a probe of dynamics in the bulk.

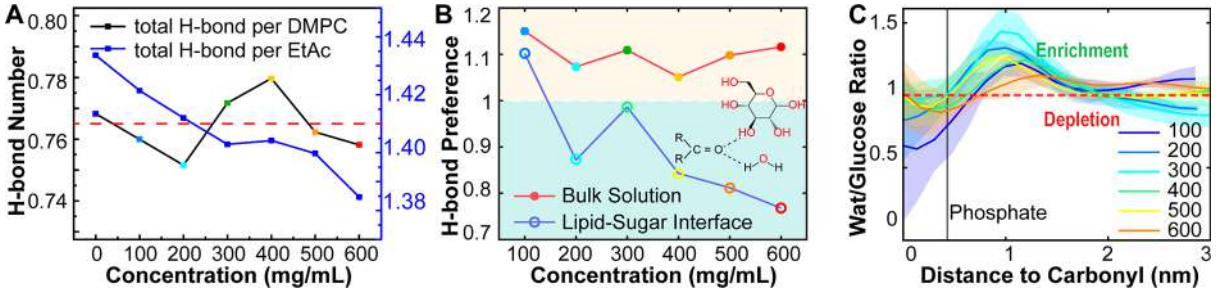

Figure 3. (A) Average numbers of H-bonds per carbonyl group extracted from MD trajectories. (B) H-Bonding preference index. This metric is obtained by dividing the carbonyl−glucose to carbonyl−water H-bond ratio in DMPC (blue) and ethyl acetate (red) by the ratio of water and glucose polar protons in each MD box (Figure S13). A value of >1 means that carbonyls preferentially H-bond to glucose; a value of <1 indicates preferential interactions with water. (C) Normalized glucose/water ratios as a function of the distance from the carbonyl groups in lipids. A value of >1 or <1 represents glucose enrichment or depletion in the region, respectively. The glucose concentrations are indicated in the inset. Shaded areas represent standard deviations over the production MD trajectory.

sugar concentration (Figure 2C). Comparing hydration structures at the interface versus bulk through MD analyses provides an atomistic interpretation of the observed trends (Section S5). The interface disrupts the extended H-bond networks of bulk water. These interfacial effects persist to a distance of ∼1 nm from the interface (Figure S19). Because DMPC lacks polar protons, water and glucose hydroxyl groups serve as the only H-bond donors. As expected, glucose decreases the number of lipid−water H-bonds but compensates for this loss by supporting additional sugar−glucose H-bonds (Figure S15) such that the overall carbonyl, as well as phosphate, H-bond population remains almost unaffected by sugar concentration (Figure 3A and Figure S16). The unchanged total number of H-bond supports the hypothesis that the environment remains largely intact, despite the very high glucose concentrations.

To more accurately assess the contributions from water and glucose H-bonds, we define an H-bond preference index. This is defined as the carbonyl−glucose/carbonyl−water H-bond ratio normalized by the number of glucose/water hydroxyl groups in the MD box (Tables S1 and S2 and Figure S13C) as shown in Figure 3B. Index values greater than unity indicate preferential interaction with glucose, and those lower than unity preferential interaction with water. Within the 100 mg/mL concentration range, the carbonyls in both DMPC and ethyl acetate exhibit slight preferential H-bonding with glucose; i.e., a value of 1.1 indicates a 10% preference for glucose (Figure 3B). However, at the interface, preferential water H-bonds are observed at increasing glucose concentrations, suggesting that lipid−water interactions remain thermodynamically favored. Surprisingly, in the bulk, preferential interactions with glucose are observed regardless of the sugar concentration. This interesting finding leads to two hypotheses. Lipids preferentially interact with water because (1) glucose is depleted at the carbonyl positions (possibly due to steric effects) or (2) glucose hydroxyl groups, while present at the interface, lack the proper orientations to strongly interact with the lipid carbonyls.

Interfacial composition is presented in terms of the distance-dependent glucose/water ratio normalized by the same ratio in the bulk, as shown in Figure 3C. Sugar is partially depleted at the carbonyl positions, while it is enriched in the region above the phosphate groups. This enrichment is likely due to steric interactions, which may prevent sugars from penetrating into the carbonyl regions, resulting in partial enrichment near the phosphate or choline groups. This enrichment shows only

https://doi.org/10.1021/acs.jpclett.1c02451
J. Phys. Chem. Lett. 2021, 12, 9602−9607

small changes with concentration, suggesting no preferential interactions between lipids and sugar. Lipid carbonyl H-bond orientational distribution functions (ODFs) further elucidate the effects of sugars on the H-bond geometries (Figure S17). Interestingly, no change in lipid water H-bond orientation is observed, and the lipid−sugar ODFs suggest that the H-bond orientations to sugars are similar to those of water throughout the concentration range, indicating that interfacial H-bond environments are unperturbed by sugars.

The H-bond populations and thermodynamics, together with the nonmonotonic H-bond time scales, indicate that the interaction at the interface is characterized by competing contributions that become dominant in different concentration regimes (Figure 2C). (1) Within the 100 mg/mL concentration range, sugars tend to "displace" water, creating unique environments, observed as a 23% deceleration of dynamics compared to those of pure water. (2) Within the intermediate concentration regime of 300−400 mg/mL, the dynamics become faster, as the carbonyls interact preferentially with water. (3) In the high-concentration range of 500−600 mg/mL, the dynamics become slower again and the bulk slows (Figure 2D). The evidence indicates that neither the "replacement" nor "displacement" hypothesis captures the effects of sugars on the interface; H-bond environments remain largely preserved, but a slight preference for water is observed at high sugar concentrations, in agreement with previous studies.[4,8,14]

In summary, 2D IR spectroscopy in combination with MD simulations was used to quantify H-bond populations, geometries, and dynamics in DMPC/sugar solutions. The studies provide strong evidence for sugar replacing water without significantly perturbing the native H-bond network at the lipid−water interface (Figure 4). The total number of lipid−water H-bonds remains stable across the entire concentration range with a slight preference for lipid−water H-bonds, in agreement with previous studies.[7,14,37,38]

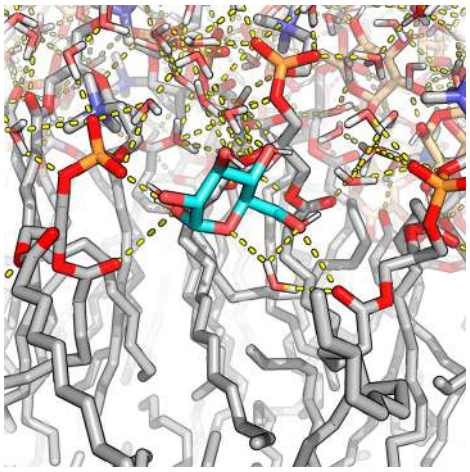

Figure 4. Snapshot of the MD trajectory showing interfacial lipid−sugar H-bonding interactions. The glucose molecule is colored cyan. Oxygens are colored red, and hydrogens are colored white. Hydrocarbon tails are colored gray.

Measured dynamics show a small variation across a large concentration range, providing further evidence that H-bond environments are largely preserved regardless of the composition of H-bonding. The reassembled H-bond network in the presence of sugar maintains the same structure as the original H-bond network at the lipid−water interface. Finally, together, our results provide evidence supporting the "replacement" hypothesis.[4,8,14] These findings improve our understanding of the sugar-induced stabilization of cell membranes under dehydration conditions. Sugar protects lipid membranes by forming a lipid−sugar−water H-bond network that is substantially similar to but perhaps more stable than the native H-bond network at the lipid−water interface in the absence of sugars.

Detailed descriptions of the experimental methods are provided in the Supporting Information (sections S1−S5). In brief, lipid samples consist of uniform ∼100 nm vesicles prepared using the sucrose solutions in D_2O to ensure uniform concentrations in the interior and exterior of the vesicles (section S1). FTIR spectra (section S2) and temperature-dependent FTIR measurements (section S3) are recorded on a Bruker Vertex 70 spectrometer. Ultrafast 2D IR experiments are measured using a custom-built setup (section S4) described previously.[39] MD simulations are carried out using the GROMACS package of programs and analyzed with Matlab (section S5).

■ ASSOCIATED CONTENT

Supporting Information

The Supporting Information is available free of charge at https://pubs.acs.org/doi/10.1021/acs.jpclett.1c02451.

Sample preparation (section S1), FTIR measurements (section S2), temperature-dependent FTIR measurements (section S3), 2D IR experiments and data (section S4), MD simulation and analysis (section S5), FTIR spectra and analysis of peak positions and areas (Figures S1−S4), 2D IR data and CLS analysis (Figures S5−S11), density profiles (Figure S12), MD simulation parameters (Figure S13), FFCF analysis (Figures S15 and S16), computation of H-bond properties (Figure S15 and Tables S1 and S2), ODF (Figure S17), radial distribution functions (Figure S18), order parameters (Figure S19), and diffusion coefficients (Figure S20) of water (PDF)

■ AUTHOR INFORMATION

Corresponding Author

Carlos R. Baiz − *Department of Chemistry, The University of Texas at Austin, Austin, Texas 78712, United States;* orcid.org/0000-0003-0699-8468; Email: cbaiz@cm.utexas.edu

Authors

Xiao You − *Department of Chemistry, The University of Texas at Austin, Austin, Texas 78712, United States;* orcid.org/0000-0002-0357-0311

Euihyun Lee − *Department of Chemistry, The University of Texas at Austin, Austin, Texas 78712, United States*

Cong Xu − *Department of Physics, The University of Texas at Austin, Austin, Texas 78712, United States*

Complete contact information is available at: https://pubs.acs.org/10.1021/acs.jpclett.1c02451

Notes

The authors declare no competing financial interest.

https://doi.org/10.1021/acs.jpclett.1c02451
J. Phys. Chem. Lett. 2021, 12, 9602−9607

■ ACKNOWLEDGMENTS

This work was supported by the National Science Foundation (CHE-1847199) and the Welch Foundation (F-1891). MD simulations were performed using the resources of the Texas Advanced Computing Center (TACC). This is a Plan II SAWIAGOS project.

■ REFERENCES

(1) Valentine, M. L.; Waterland, M. K.; Fathizadeh, A.; Elber, R.; Baiz, C. R. Interfacial Dynamics in Lipid Membranes: The Effects of Headgroup Structures. *J. Phys. Chem. B* **2021**, *125* (5), 1343−1350.
(2) Crowe, J. H.; Hoekstra, F. A.; Crowe, L. M. Anhydrobiosis. *Annu. Rev. Physiol.* **1992**, *54* (1), 579−599.
(3) Roy, A.; Dutta, R.; Kundu, N.; Banik, D.; Sarkar, N. A Comparative Study of the Influence of Sugars Sucrose, Trehalose, and Maltose on the Hydration and Diffusion of DMPC Lipid Bilayer at Complete Hydration: Investigation of Structural and Spectroscopic Aspect of Lipid-Sugar Interaction. *Langmuir* **2016**, *32* (20), 5124−34.
(4) Stachura, S. S.; Malajczuk, C. J.; Mancera, R. L. Does Sucrose Change Its Mechanism of Stabilization of Lipid Bilayers during Desiccation? Influences of Hydration and Concentration. *Langmuir* **2019**, *35* (47), 15389−15400.
(5) Ohtake, S.; Schebor, C.; Palecek, S. P.; de Pablo, J. J. Effect of sugar-phosphate mixtures on the stability of DPPC membranes in dehydrated systems. *Cryobiology* **2004**, *48* (1), 81−9.
(6) Pereira, C. S.; Hunenberger, P. H. Interaction of the sugars trehalose, maltose and glucose with a phospholipid bilayer: a comparative molecular dynamics study. *J. Phys. Chem. B* **2006**, *110* (31), 15572−81.
(7) Crowe, J. H.; Whittam, M. A.; Chapman, D.; Crowe, L. M. Interactions of phospholipid monolayers with carbohydrates. *Biochim. Biophys. Acta, Biomembr.* **1984**, *769* (1), 151−9.
(8) Leonov, D. V.; Dzuba, S. A.; Surovtsev, N. V. Membrane-Sugar Interactions Probed by Low-Frequency Raman Spectroscopy: The Monolayer Adsorption Model. *Langmuir* **2020**, *36* (39), 11655−11660.
(9) Crowe, J. H.; Crowe, L. M.; Chapman, D. Preservation of membranes in anhydrobiotic organisms: the role of trehalose. *Science* **1984**, *223* (4637), 701−3.
(10) Villarreal, M. A.; Diaz, S. B.; Disalvo, E. A.; Montich, G. G. Molecular dynamics simulation study of the interaction of trehalose with lipid membranes. *Langmuir* **2004**, *20* (18), 7844−51.
(11) Sun, W. Q.; Leopold, A. C.; Crowe, L. M.; Crowe, J. H. Stability of dry liposomes in sugar glasses. *Biophys. J.* **1996**, *70* (4), 1769−76.
(12) Elbein, A. D.; Pan, Y. T.; Pastuszak, I.; Carroll, D. New insights on trehalose: a multifunctional molecule. *Glycobiology* **2003**, *13* (4), 17R−27R.
(13) Weng, L.; Ziaei, S.; Elliott, G. D. Effects of Water on Structure and Dynamics of Trehalose Glasses at Low Water Contents and its Relationship to Preservation Outcomes. *Sci. Rep.* **2016**, *6* (1), 28795.
(14) Andersen, H. D.; Wang, C.; Arleth, L.; Peters, G. H.; Westh, P. Reconciliation of opposing views on membrane-sugar interactions. *Proc. Natl. Acad. Sci. U. S. A.* **2011**, *108* (5), 1874−8.
(15) Cordone, L.; Cottone, G.; Giuffrida, S. Role of residual water hydrogen bonding in sugar/water/biomolecule systems: a possible explanation fortrehalose peculiarity. *J. Phys.: Condens. Matter* **2007**, *19* (20), 205110.
(16) Golovina, E. A.; Golovin, A. V.; Hoekstra, F. A.; Faller, R. Water replacement hypothesis in atomic detail–factors determining the structure of dehydrated bilayer stacks. *Biophys. J.* **2009**, *97* (2), 490−499.
(17) Golovina, E. A.; Golovin, A.; Hoekstra, F. A.; Faller, R. Water Replacement Hypothesis in Atomic Details: Effect of Trehalose on the Structure of Single Dehydrated POPC Bilayers. *Langmuir* **2010**, *26* (13), 11118−11126.
(18) Tsvetkova, N. M.; Phillips, B. L.; Crowe, L. M.; Crowe, J. H.; Risbud, S. H. Effect of sugars on headgroup mobility in freeze-dried dipalmitoylphosphatidylcholine bilayers: solid-state 31P NMR and FTIR studies. *Biophys. J.* **1998**, *75* (6), 2947−55.
(19) Lambruschini, C.; Relini, A.; Ridi, A.; Cordone, L.; Gliozzi, A. Trehalose Interacts with Phospholipid Polar Heads in Langmuir Monolayers. *Langmuir* **2000**, *16* (12), 5467−5470.
(20) Kent, B.; Garvey, C. J.; Lenné, T.; Porcar, L.; Garamus, V. M.; Bryant, G. Measurement of glucose exclusion from the fully hydrated DOPE inverse hexagonal phase. *Soft Matter* **2010**, *6* (6), 1197−1202.
(21) Lenné, T.; Bryant, G.; Garvey, C. J.; Keiderling, U.; Koster, K. L. Location of sugars in multilamellar membranes at low hydration. *Phys. B* **2006**, *385*, 862−864.
(22) Soderlund, T.; Alakoskela, J. M.; Pakkanen, A. L.; Kinnunen, P. K. Comparison of the effects of surface tension and osmotic pressure on the interfacial hydration of a fluid phospholipid bilayer. *Biophys. J.* **2003**, *85* (4), 2333−41.
(23) Flanagan, J. C.; Valentine, M. L.; Baiz, C. R. Ultrafast Dynamics at Lipid-Water Interfaces. *Acc. Chem. Res.* **2020**, *53* (9), 1860−1868.
(24) Kundu, A.; Verma, P. K.; Ha, J. H.; Cho, M. Studying Water Hydrogen-Bonding Network near the Lipid Multibilayer with Multiple IR Probes. *J. Phys. Chem. A* **2017**, *121* (7), 1435−1441.
(25) Lee, E.; Kundu, A.; Jeon, J.; Cho, M. Water hydrogen-bonding structure and dynamics near lipid multibilayer surface: Molecular dynamics simulation study with direct experimental comparison. *J. Chem. Phys.* **2019**, *151* (11), 114705.
(26) Bhattacharyya, K. Nature of biological water: a femtosecond study. *Chem. Commun. (Cambridge, U. K.)* **2008**, No. 25, 2848−57.
(27) Baiz, C. R.; Blasiak, B.; Bredenbeck, J.; Cho, M.; Choi, J. H.; Corcelli, S. A.; Dijkstra, A. G.; Feng, C. J.; Garrett-Roe, S.; Ge, N. H.; Hanson-Heine, M. W. D.; Hirst, J. D.; Jansen, T. L. C.; Kwac, K.; Kubarych, K. J.; Londergan, C. H.; Maekawa, H.; Reppert, M.; Saito, S.; Roy, S.; Skinner, J. L.; Stock, G.; Straub, J. E.; Thielges, M. C.; Tominaga, K.; Tokmakoff, A.; Torii, H.; Wang, L.; Webb, L. J.; Zanni, M. T. Vibrational Spectroscopic Map, Vibrational Spectroscopy, and Intermolecular Interaction. *Chem. Rev.* **2020**, *120* (15), 7152−7218.
(28) Valentine, M. L.; Cardenas, A. E.; Elber, R.; Baiz, C. R. Physiological Calcium Concentrations Slow Dynamics at the Lipid-Water Interface. *Biophys. J.* **2018**, *115* (8), 1541−1551.
(29) Flanagan, J. C.; Cardenas, A. E.; Baiz, C. R. Ultrafast Spectroscopy of Lipid-Water Interfaces: Transmembrane Crowding Drives H-Bond Dynamics. *J. Phys. Chem. Lett.* **2020**, *11* (10), 4093−4098.
(30) Costard, R.; Heisler, I. A.; Elsaesser, T. Structural Dynamics of Hydrated Phospholipid Surfaces Probed by Ultrafast 2D Spectroscopy of Phosphate Vibrations. *J. Phys. Chem. Lett.* **2014**, *5* (3), 506−11.
(31) Edington, S. C.; Flanagan, J. C.; Baiz, C. R. An Empirical IR Frequency Map for Ester C horizontal lineO Stretching Vibrations. *J. Phys. Chem. A* **2016**, *120* (22), 3888−96.
(32) Lewis, R. N. A. H.; McElhaney, R. N. The structure and organization of phospholipid bilayers as revealed by infrared spectroscopy. *Chem. Phys. Lipids* **1998**, *96* (1−2), 9−21.
(33) Rosa, A. S.; Disalvo, E. A.; Frias, M. A. Water Behavior at the Phase Transition of Phospholipid Matrixes Assessed by FTIR Spectroscopy. *J. Phys. Chem. B* **2020**, *124* (29), 6236−6244.
(34) Binder, H. Water near lipid membranes as seen by infrared spectroscopy. *Eur. Biophys. J.* **2007**, *36* (4−5), 265−79.
(35) Venkatraman, R. K.; Baiz, C. R. Ultrafast Dynamics at the Lipid-Water Interface: DMSO Modulates H-Bond Lifetimes. *Langmuir* **2020**, *36* (23), 6502−6511.
(36) Telis, V. R. N.; Telis-Romero, J.; Mazzotti, H. B.; Gabas, A. L. Viscosity of Aqueous Carbohydrate Solutions at Different Temperatures and Concentrations. *Int. J. Food Prop.* **2007**, *10* (1), 185−195.
(37) Strauss, G.; Schurtenberger, P.; Hauser, H. The interaction of saccharides with lipid bilayer vesicles: stabilization during freeze-thawing and freeze-drying. *Biochim. Biophys. Acta, Biomembr.* **1986**, *858* (1), 169−80.
(38) Kapla, J.; Wohlert, J.; Stevensson, B.; Engström, O.; Widmalm, G.; Maliniak, A. Molecular Dynamics Simulations of Membrane−Sugar Interactions. *J. Phys. Chem. B* **2013**, *117* (22), 6667−6673.

https://doi.org/10.1021/acs.jpclett.1c02451
J. Phys. Chem. Lett. 2021, 12, 9602−9607

(39) Oh, K. I.; You, X.; Flanagan, J. C.; Baiz, C. R. Liquid-Liquid Phase Separation Produces Fast H-Bond Dynamics in DMSO-Water Mixtures. *J. Phys. Chem. Lett.* **2020**, *11* (5), 1903−1908.

https://doi.org/10.1021/acs.jpclett.1c02451
J. Phys. Chem. Lett. 2021, 12, 9602−9607